Pacific Northwest
NATIONAL LABORATORY

PNNL-35370

Characterizing Interference in a Wave-Powered Buoy

April 2024

Ruth Branch
Rob Cavagnaro
Ben Roberts
James McVey
Alex Barker
Alex Turpin

U.S. DEPARTMENT OF ENERGY

Prepared for the U.S. Department of Energy
Under contract DE-AC05-76RL01830

DISCLAIMER

This report was prepared as an account of work sponsored by an agency of the United States Government. Neither the United States Government nor any agency thereof, nor Battelle Memorial Institute, nor any of their employees, **makes any warranty, express or implied, or assumes any legal liability or responsibility for the accuracy, completeness, or usefulness of any information, apparatus, product, or process disclosed, or represents that its use would not infringe privately owned rights**. Reference herein to any specific commercial product, process, or service by trade name, trademark, manufacturer, or otherwise does not necessarily constitute or imply its endorsement, recommendation, or favoring by the United States Government or any agency thereof, or Battelle Memorial Institute. The views and opinions of authors expressed herein do not necessarily state or reflect those of the United States Government or any agency thereof.

PACIFIC NORTHWEST NATIONAL LABORATORY
operated by
BATTELLE
for the
UNITED STATES DEPARTMENT OF ENERGY
under Contract DE-AC05-76RL01830

Printed in the United States of America

Available to DOE and DOE contractors from the Office of Scientific and Technical Information,
P.O. Box 62, Oak Ridge, TN 37831-0062
www.osti.gov
ph: (865) 576-8401
fax: (865) 576-5728
email: reports@osti.gov

Available to the public from the National Technical Information Service
5301 Shawnee Rd., Alexandria, VA 22312
ph: (800) 553-NTIS (6847)
or (703) 605-6000
email: info@ntis.gov
Online ordering: http://www.ntis.gov

PNNL-35370

Characterizing Interference in a Wave-Powered Buoy

April 2024

Ruth Branch
Rob Cavagnaro
Ben Roberts
James McVey
Alex Barker
Alex Turpin

Prepared for
the U.S. Department of Energy
Under Contract DE-AC05-76RL01830

Pacific Northwest National Laboratory
Richland, Washington 99352

Executive Summary

Oceanographic measurement buoys are power constrained by the capacity of their batteries and limited area or resource for solar power. Many buoys are in locations with abundant wave energy, but wave energy converters are not being used to power them. One reason wave energy converters have not been developed for wave measurement buoys is because many buoys measure waves by precisely following the wave motion. Wave energy converters may inhibit this wave-following ability by altering a buoy's response to incoming waves. In this report, we present the results of field tests that measured the extent to which buoy motion was changed by modifications to the buoy for wave energy harvesting. The motion of the buoy was significantly modified by the addition of the hardware components necessary for harvesting wave energy. The ratio of the wave energy converter's mass to the buoy's mass was high for the system tested, which strongly affected buoy motion. A lower ratio would decrease the effect of the wave energy converter on the motion of the buoy, thereby decreasing the impact on the buoy's ability to measure waves, but a lower ratio would also decrease the wave energy converter's ability to produce power. A low ratio can be achieved by using a large buoy and a small wave energy converter. Buoy size constrains the wave measurement to only waves large enough to alter the buoy motion. Therefore, the use of wave energy converters to power wave measurement buoys may be feasible for large buoys that measure low-frequency waves if the affects of the wave energy converter motion have been accounted for in wave parameter calculations.

Acronyms and Abbreviations

CDIP	Coastal Data Information Program
DoF	degree of freedom
FFT	fast Fourier transform
GPS	global positioning system
IMU	inertial measurement unit
IRM	internal reaction mass
NDBC	National Data Buoy Center
PG	Pacific Gyre
rPi	Raspberry Pi
WEC	wave energy converter
WITT	Whatever Input to Torsion Transfer

Acknowledgments

This work is funded by the U.S. Department of Energy, Office of Energy Efficiency and Renewable Energy, Water Power Technologies Office under contract DE-AC05-76RL01830 to Pacific Northwest National Laboratory.

Contents

Figures

Tables

1.0 Introduction

Hundreds of moored and drifting buoys measure waves for assimilation to weather forecast models, oceanographic studies, and monitoring for coastal communities. The buoys are operated by government organizations such as the National Data Buoy Center (NDBC) and the Coastal Data Information Program (CDIP), university laboratories, and indigenous communities such as the Backyard Buoys project (www.pacioos.hawaii.edu/projects/backyard-buoys/). Buoy sizes range from handheld Spotter buoys (www.sofarocean.com) to 12 m wide NDBC buoys, and all are dependent on battery storage or solar panels. The quantity of measurements that buoys are able to make and the length of time that they can operate are constrained by the power capacity of the solar panels and batteries. Electricity generated by wave energy converters (WECs) on the buoys could be used to recharge batteries, increase the frequency of measurements, and extend the lifetime of the buoys (Cavagnaro et al. 2020).

A subset of wave energy converter technologies can be described as internal reaction mass (IRM) technologies, where mechanical energy is harvested from the waves by a moving mass in the WEC structure. These technologies can be divided into device categories of a sliding mass, pendulum, or gyroscope (Kenny and McNally 2022). A sliding mass device has a mass that translates linearly; a pendulum device has a mass that rotates irregularly around an axis; and a gyroscope device has a mass that spins continuously. Here, we describe a test where a pendulum device is added to a buoy to create a WEC that converts the mechanical energy harvested from waves into electrical power. The motion of the buoy is monitored and compared to the motion of a second buoy with a comparable mass but no moving WEC parts. The movement of the two buoys is analyzed to determine if the buoys can be used to accurately measure waves.

Buoy size fundamentally determines the size (i.e., wavelength) of the waves that a wave-following buoy can measure. This limitation is based on whether or not the buoy's frequency response (i.e., amplitude of motion as a function of excitation frequency) overlaps with the wave motion it experiences. If the waves are significantly smaller than the buoy, the buoy will tend not to respond to the wave motion and therefore can't measure that size of the wave. Smaller spherical buoys have higher natural frequencies than larger ones. For example, the Sofar Spotter has a natural frequency of 1.2 Hz, so the maximum wave frequency it records is slightly lower at 1 Hz (Raghukumar et al. 2019). Larger buoys like NDBC buoys (3, 10, or 12 m diameter) are configured to record waves with wave periods longer than 3 s (14 m wavelength), but smaller buoys like the Datawell WaveRider 3 (0.7 or 0.9 m diameter, used in the modern CDIP) or Sofar Spotter v2 (0.42 $\times$ 0.31 m) buoys measure waves with wave periods as small as 1.6 and 1 s (1.5 m wavelength), respectively (Cotter and McVey 2021). Buoy size affects the accuracy of the measured wave height; the accuracy of the wave heights measured by Sofar Spotter wave buoys is an order of magnitude higher than that measured by NDBC buoys (0.02 and 0.2 m, respectively). The nonspherical shape and wave instrument configurations of NDBC buoys require the significant use of transfer functions to retain high-quality bulk and directional wave estimates, which are tuned to deployment locations and wave states (Teng 2002). Because they're derived empirically, the use of transfer functions will increase the uncertainty of wave measurements that rely on them. If the mass of the moving parts in the WEC is significant in comparison to the mass of the buoy, the momentum of the moving WEC parts is likely to change how the buoy moves in response to the forcing from the waves, therefore reducing its measurement accuracy. This report describes a test designed to measure the change in motion of an industry-relevant ocean sensor buoy when components enabling wave energy harvesting are added to it.

2.0 Buoy Design

To test the hypothesis that the integration of a WEC with a wave buoy affects buoy motion and therefore its ability to measure waves, we modified and tested two Pacific Gyre (PG) Universal Tracker buoys. A prototype WEC, the "Whatever Input to Torsion Transfer" (WITT; WITT Energy, United Kingdom), was installed in one of the buoys (hereafter WEC-buoy), while stationary ballast of equal mass was installed in the other buoy (hereafter no WEC-buoy). Both buoys were tethered with rubber shock cord to heave plates to provide a reaction force for the system's buoyancy and the WITT's IRM technology. The Universal Tracker buoys tested here have an elongated spherical shell (Fig. 1) with an outside diameter of 0.46 m (18 in.) and a height of 0.56 m (22 in.).

The WITT itself is an energy harvesting device that uses a unique gearbox and pendulum system to rectify motion in six degrees of freedom (DoFs) to one DoF, rotating a shaft (Crowley et al. 2018; Wickett et al. 2019). This particular prototype had two pendulums with masses of 2.77 and 2.78 kg that rotated within the volume of a 0.28 m diameter sphere. The WITT was mounted inside the buoy by attaching its two connection points to rings that were clamped to the flange of the buoy's upper section (Fig. 2). The pendulum transmission system and electronics were mounted in the buoy such that pendulum movement was not restricted.

Prior to modification, the two buoys were identical, and each had a mass of 11.1 kg. Mounting rings were installed in both buoys. The WITT pendulums, which contain the majority of the WITT's weight, had a combined mass of 5.5 kg, and the stationary weights used in the other buoy had a mass of 6.8 kg. The mounting hardware for the WITT and stationary weights varied slightly and another 6.8 kg was added to the bottom of both buoys as ballast. The total mass of the buoy with the WITT mounted in it was 34.6 kg, and the total mass of the buoy with the stationary weights was 35.1 kg. Figure 3 shows photos of the interiors of the two buoys. The integrated WITT pendulum IRM is mounted in the WEC-buoy and the a dummy payload of weights is mounted in the no WEC-buoy.

For instrumentation, an inertial measurement unit (IMU; Yost TSS-USB-S v2.1e), global positioning system (GPS; Adafruit PA161S), and Raspberry Pi (rPi) microcontroller were mounted in each buoy to measure and acquire buoy motion and position data. A subsection of the University of Washington Applied Physics Lab's MicroSWIFT code (https://github.com/SASlabgroup/microSWIFT) was installed onto the rPi to record IMU and GPS data. Bulk wave statistics were calculated from the IMU data following the methods listed in Cotter and McVey (2021).

Figure 1. Pacific Gyre elongated spherical buoy.

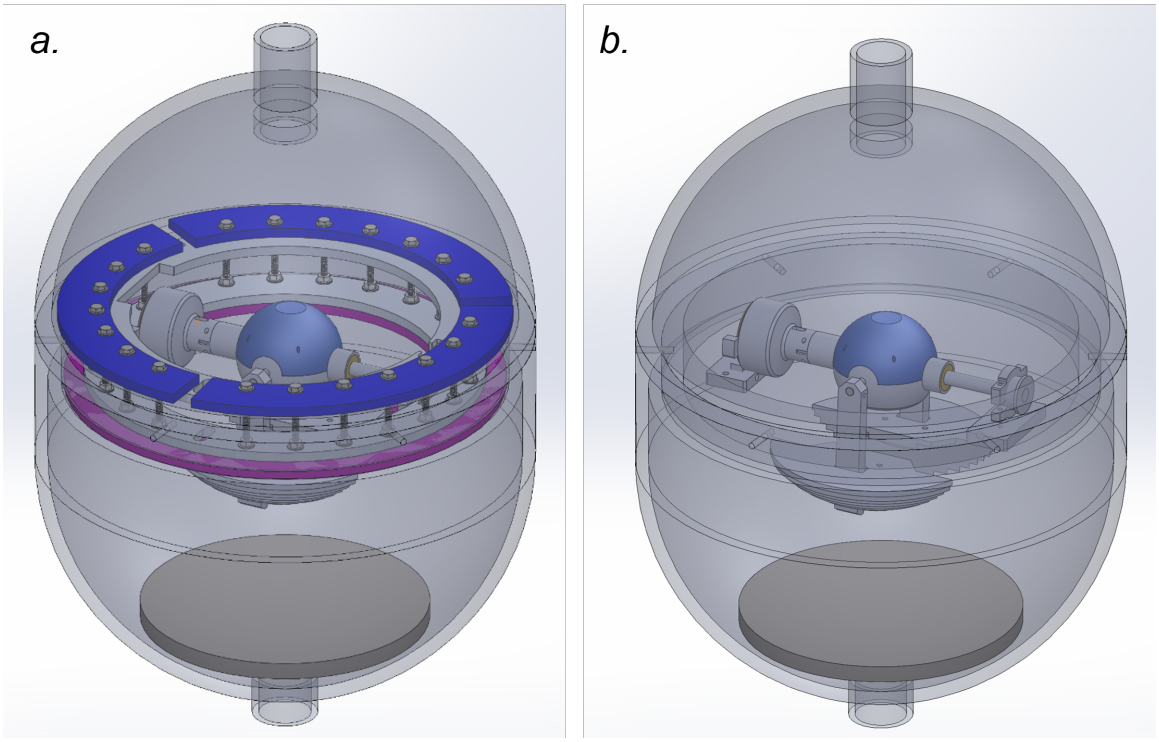

Figure 2. Engineering drawing of the WITT mounted within the PG buoy. The buoy separates into two halves and is joined by bolting the flange on the upper section to the rim of the lower. (a) The buoy interior is shown with the ring clamps highlighted in blue and purple. (b) The buoy interior is shown with the clamp hardware hidden to reveal the pendulums hanging beneath the blue gearbox enclosure.

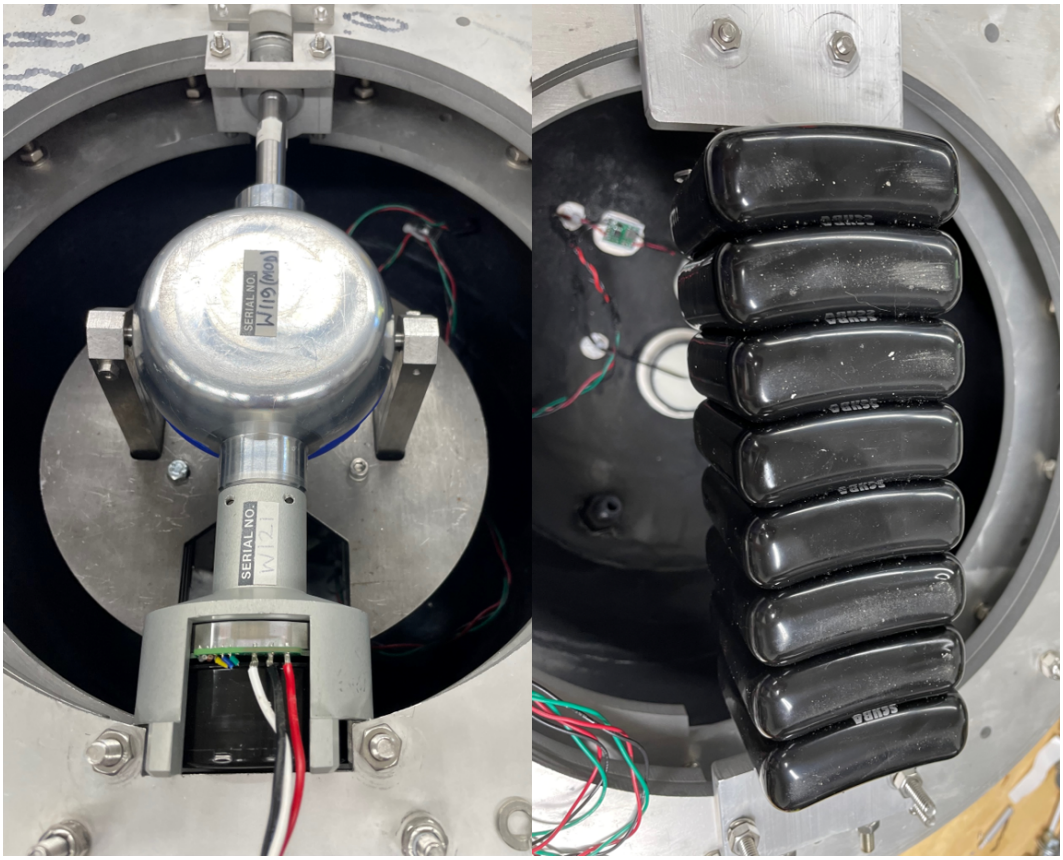

Figure 3. Interiors of the WEC-buoy (left) and no WEC-buoy (right). The WITT pendulums are the half circles hanging from the gearbox and the stationary weights are mounted across the interior of the no WEC-buoy.

Heave plates made of high density polyethylene were used to provide a reaction force against the system's buoyancy and the wave forces acting on the buoys at the surface (Fig. 4). When the buoy was displaced by a wave, it pulled against the tether connecting it to the relatively stationary heave plate. The heave plate, which has high drag and added mass, resisted this wave force. Consequently, the buoy was then forced to absorb some of this passing wave energy, causing the WITT pendulums to swing and produce electricity. The heave plates had a mass of 2 kg, a diameter of 0.51 m, and a height of 0.01 m. They were tethered to the underside of the buoys with 2 m long rubber cords and 0.41 m four-line Amsteel bridles. Rubber cords were used to reduce the shock impact on the buoys' tether joints. The heave plates themselves were positively buoyant (+0.23 kg), and 2 kg weights were attached to the bridles beneath them to provide a downward restoring force.

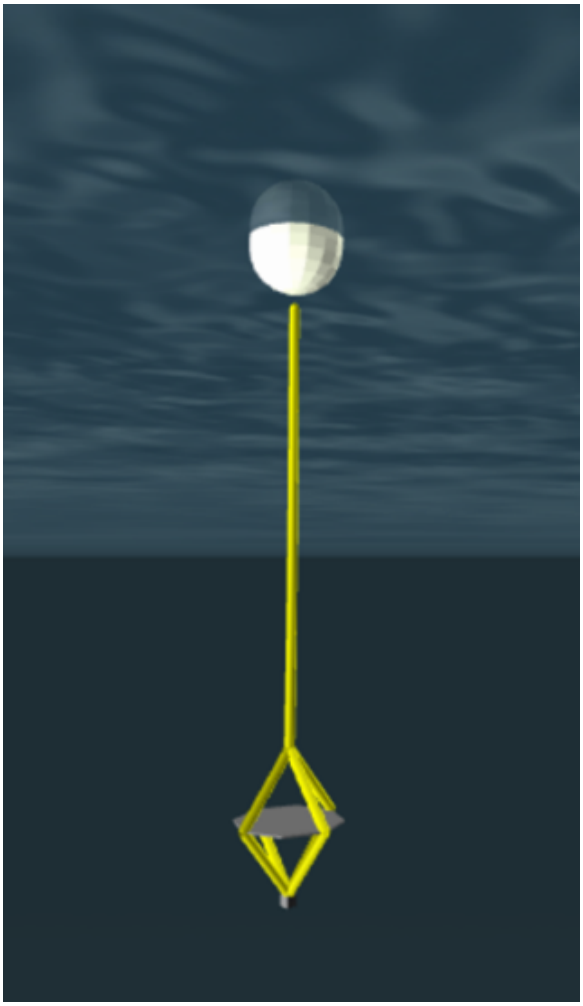

Figure 4. Model of a PG buoy with the heave plate tether.

3.0 Buoy Field Tests

Several field tests were conducted to compare the motion of the WEC-buoy and the no WEC-buoy. The external weight and heave plate configurations were varied in the tests to determine which configuration generated the most buoy motion. The external weight and heave plate configurations were identical for both the WEC-buoy and no WEC-buoy during the tests. The tests were conducted in quiescent water in Sequim Bay, WA, and under natural wave conditions in the Strait of Juan de Fuca near PNNL-Sequim. A boat was used to generate waves in Sequim Bay. In each of the tests, both buoys were set adrift freely for up to one hour alongside a Sofar Spotter 3 buoy, which measured the ambient wave conditions. All three buoys were released from the boat at the same time and location (Fig. 5). They were allowed to drift during the tests but were not more than 50 m apart at any given time.

Figure 5. The WEC-buoy (left top), no WEC-buoy (right), and Sofar Ocean Spotter 3 buoy (left bottom) during a field test.

A total of six field tests were conducted on three separate days (Table 1). The field test on July 28, 2023 took place outside Sequim Bay under natural wave conditions. The tests on August 14, 2023 took place inside Sequim Bay with the boat driving in circles around the buoys to expose them to a boat wake. The final test on September 7, 2023 took place outside Sequim Bay under natural wave conditions. The wave conditions varied from significant wave heights (H_s) of 0.24 m to 0.47 m and peak wave periods (T_p) from 2.2 s to 15 s.

Table 1. Buoy configurations and wave conditions during field tests. The waves are denoted as wind waves (W) or boat wakes (B).

Test	Date	Waves	Heave Plate	Weight (kg)	H_s (m)	T_p (s)
1	28 Jul 2023	W	✓	2.27	0.43	3.3
2	14 Aug 2023	B		4.54	0.25	8.7
3	14 Aug 2023	B	✓	0	0.33	2.2
4	14 Aug 2023	B		0	0.24	8.5
5	7 Sep 2023	W	✓	0	0.24	15
6	7 Sep 2023	W	✓	0	0.47	9.4

The buoys were tested under a variety of weight and heave plate conditions to identify the configuration that maximized the tilt and acceleration responses to the waves (Table 1). During the tests, the WEC-buoy and no WEC-buoy had identical heave plate/external weight configurations. The test on July 28, 2023 was conducted with the heave plates attached and 2.27 kg of external weight on each buoy (Fig. 6a). The WEC-buoy was too stable in that configuration to initiate a significant amount of motion of the pendulums. Three configurations were tested on August 14, 2023 (Table 1). The buoys were first deployed without the heave plates and with 4.54 kg of external weight (Fig. 6b). The external weight was then removed, and the heave plates were attached (Fig. 6c). The final test on August 14, 2023 was conducted without the heave plates or external weight (Fig. 6d). The tests on September 7, 2023 were conducted to measure the buoy movement and power produced in wind-generated waves with the heave plate and no external weight (Fig. 6c).

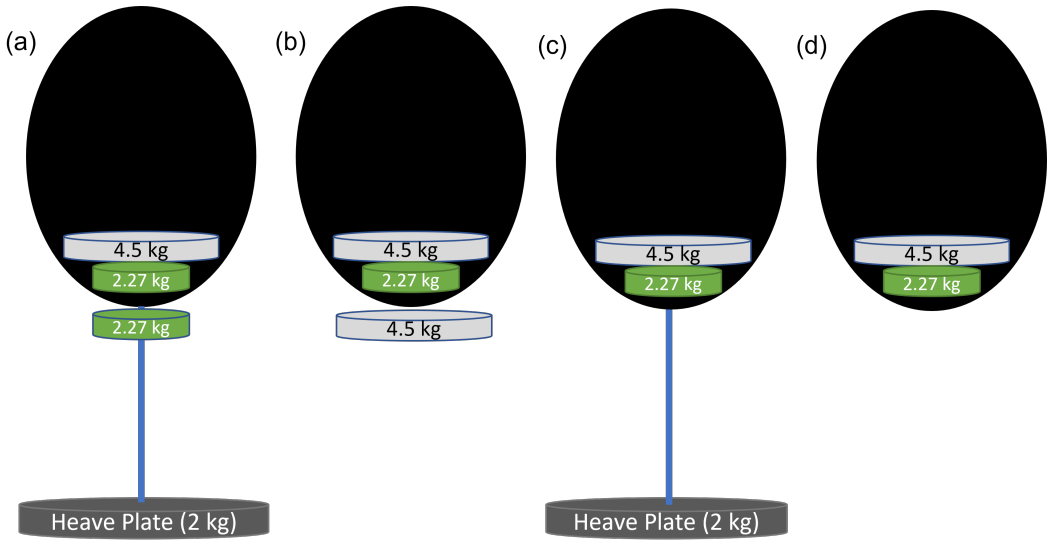

Figure 6. Buoy test configurations. a) Test 1: heave plate and 2.27 kg b) Test 2: no heave plate and 4.5 kg c) Tests 3,5,6: heave plate and no external weight d) Test 4: no heave plate and no external weight

4.0 Buoy Motion Analysis

Buoy motion was tracked for all three buoys to compare the movement of the PG buoys to the Spotter 3 buoy. Displacement (X, Y, Z) and GPS (latitude, longitude) data were collected by the Spotter 3 buoy at 2.5 Hz. IMU data (accelerometer and quaternion) and GPS (latitude, longitude) data were collected at 4 Hz via the microSWIFT code on the rPi devices in the PG buoys. Pitch, roll, and yaw were calculated from the quaternion data, which were used to correct the accelerometer vector to constrain the gravity vector to the Z direction. When the buoy tilted, a component of the gravitational force was recorded along the X and Y axes of the acceleration vector. Sensor drift was calculated using a low-pass Butterworth filter (2nd order, with a cutoff frequency of 0.0455 Hz) and subtracted from the acceleration vector, which was integrated to find the velocity vector. The energy spectrum was calculated from the vertical velocity using the Python package MHKiT (Klise et al. 2020) with a Hanning window and a fast Fourier transform (FFT) length equal to 1/3 of the bin size. The Spotter 3 buoy records displacement measurements in the Cartesian (X, Y, Z) coordinate frame (Raghukumar et al. 2019). The wave energy spectrum was directly calculated from the Spotter 3 vertical (Z) position data.

Energy spectra can be used to compare the motions of the three buoys during the six field tests (Fig. 7). The spectra show that the no WEC-buoy and WEC-buoy generally had similar responses at frequencies higher than 0.5 Hz, but the WEC-buoy almost always exhibited attenuation compared with the no WEC-buoy at lower frequencies (<0.5 Hz) for all tests. The decrease in the energy of the WEC-buoy is due to a decrease in the vertical motion (heave response) as compared to the no-WEC buoy. This implies that the WITT in the WEC-buoy decreased the motion of the buoy by extracting energy and converting it to pendulum motion. The average difference of the energy spectra integrated across a frequency band of 0.05-1 Hz between the no WEC-buoy and the WEC-buoy, ΔE, is calculated as

$$\Delta E = \int_{0.05}^{1} E_{noWEC} - E_{WEC}\, df \tag{1}$$

and shown in Table 2. The maximum energy was extracted by the WEC-buoy during Test 6, which was also the test with the largest theoretical wave energy, J, based on H_s and T_p. The minimum energy was extracted by the WEC-buoy during Test 1, which was not the test with the lowest value of the theoretical wave energy, but the test with the external weight and heave plate configuration that may have stabilized it (i.e., an unfavorable configuration for energy harvesting). Tests 2 through 5 don't show a pattern between the theoretical wave energy value and the difference between the energy spectra, but the changing heave plate and weight conditions may have influenced the variability in the energy transfer between the waves and the buoys.

Table 2. Wave parameters, theoretical wave energy per crest length, J, the integrated difference in the energy spectra, ΔE, and the integrated difference in the transfer function, ΔT, between the no WEC-buoy and the WEC-buoy.

Test	H_s (m)	T_p (s)	J (W/m)	ΔE (m^2)	ΔT (Hz)
1	0.43	3.3	254	0.0051	0.99
2	0.25	8.7	226	0.0369	14.63
3	0.33	2.2	100	0.0624	44.49
4	0.24	8.5	204	0.0581	21.03
5	0.24	15	359	0.0448	21.58
6	0.47	9.4	863	0.1520	13.61

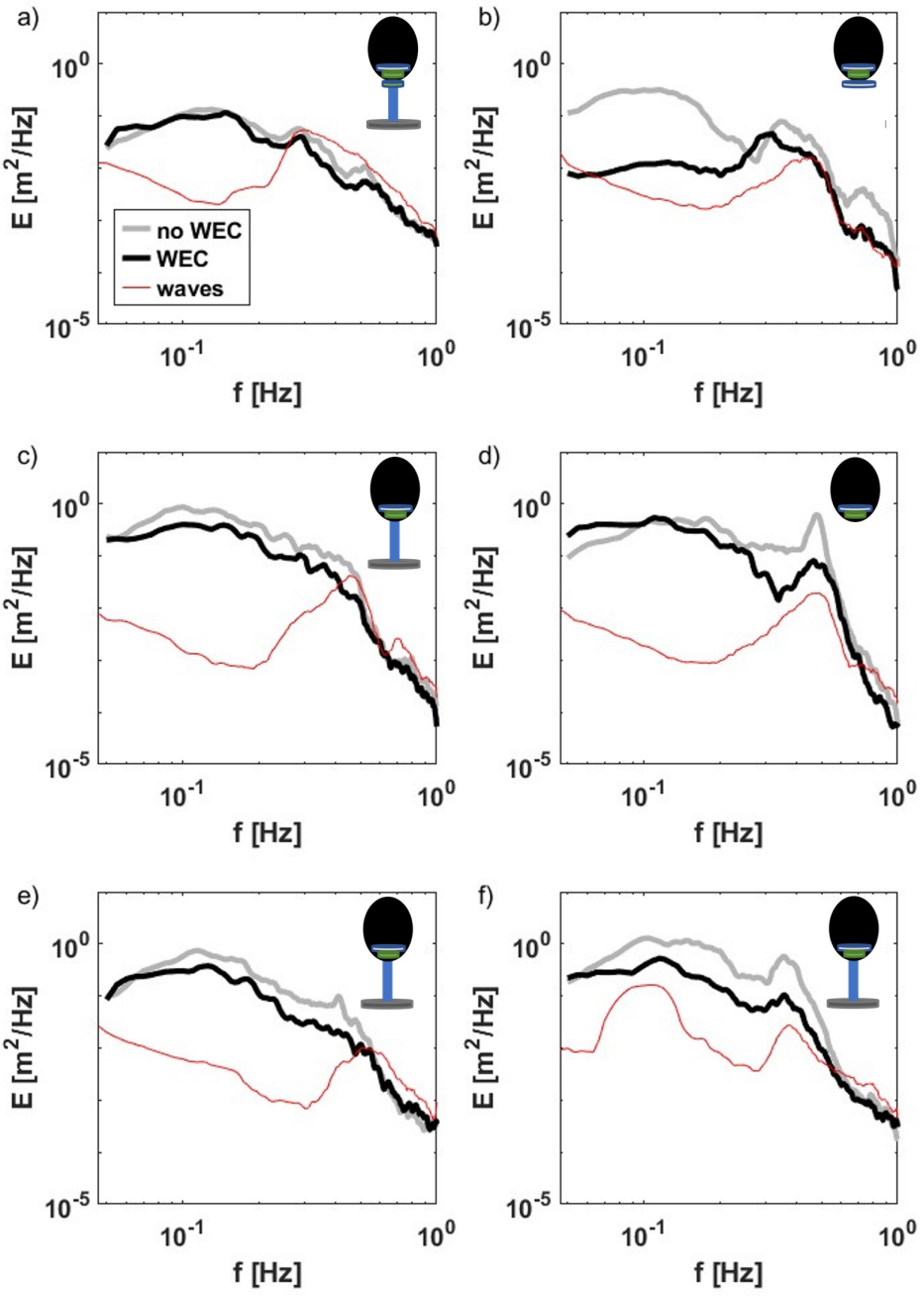

Figure 7. Energy spectra, E, for the buoy with no WEC, the buoy with the WEC, and the waves as measured by the Spotter buoy. The buoy diagrams show the weight and heave plate configurations for each test. a) Test 1 on July 28, b) Test 2 on August 14, c) Test 3 on August 14, d) Test 4 on August 14, e) Test 5 on September 7, and f) Test 6 on September 7.

Bulk wave parameters such as H_s and T_p were calculated from the wave spectra using MHKiT for all three buoys (Klise et al. 2020). The wave parameters measured by the Spotter 3 buoy were compared to those measured by the PG buoys to determine how well the PG buoys measured waves without the implementation of a transfer function to correct for imperfect wave following motion of the buoys. The significant wave heights calculated from the PG buoys were higher than the H_s values measured by the Spotter 3 buoy in all tests (Table 3). The estimate of H_s depends on the amount of energy in the vertical spectrum, which indicates that the PG buoy was experiencing excess vertical motion (bobbing) beyond that of the waves. The wave heights calculated from the no WEC-buoy were higher than those calculated with data from the WEC-buoy, which implies that the extraction of energy by the WITT decreased the excess vertical motion. The H_s values were most similar between the three buoys during Test 1. Therefore, the configuration of Test 1 (heave plate + 2.27 kg) was the configuration where the PG buoys were most closely following the waves.

The peak wave period was calculated from the maximum frequency peak in the vertical spectrum. The Spotter 3 buoy measured a peak wave period of 3.3 s during Test 1 (Table 3). The wave periods measured by the Spotter 3 buoys during Tests 2–4 are estimates because of the nonsinusoidal nature of boat wakes. The Spotter 3 buoy measured peak wave periods of 15 and 9.4 s for Tests 5 and 6, respectively, and the spectra also showed significant wind wave peaks around 2–3 s (0.3–0.5 Hz) (Fig. 7). The peak periods calculated with the PG motion data did not agree well with the Spotter 3 values for any of the tests (Table 3). This result implies that the buoys as designed were not adequate wave followers for wave measurement and that the addition of transfer functions would be required to obtain accurate wave measurements.

Table 3. Estimates of H_s and T_p from field tests of three buoys.

Test	Waves or Boat Wakes	Spotter 3 H_s (m)	no WEC-buoy H_s (m)	WEC-buoy H_s (m)	Spotter 3 T_p (s)	no WEC-buoy T_p (s)	WEC-buoy T_p (s)
1	W	0.43	0.67	0.53	3.3	7.4	7.6
2	B	0.25	0.84	0.37	8.7	10.4	3.3
3	B	0.33	1.4	1.0	2.2	9.5	9.7
4	B	0.24	1.5	1.1	8.5	3.3	10.2
5	W	0.24	1.2	0.87	15	8.2	10.5
6	W	0.47	1.9	0.97	9.4	7.9	10.6

Buoy motion was further examined by calculating the transfer function, T, between the motion of the waves and the motion of the WEC-buoy and no WEC-buoy. The transfer function shows the relative response of each buoy to the input wave energy. It is defined as the ratio of the spectrum of the motion of the buoy to the spectrum of the motion of the waves.

$$T = E_{buoy}/E_{waves} \tag{2}$$

The spectra of the motion of the waves, E_{waves}, was measured by the Sofar Ocean Spotter 3 buoy and shown as the wave energy spectra on Figure 7. The spectra of the motion of the WEC-buoy and the no WEC-buoy were calculated from vertical velocity data obtained from the IMUs that were mounted in the buoys. The transfer functions were lower for the WEC-buoy than the no WEC-buoy for most tests and wavelengths (Fig. 8). The decrease in the transfer

function shows that the WEC-buoy is less responsive to the wave energy and is therefore less capable of measuring the waves unless the decrease is characterized and accounted for under all relevant conditions. The integrated difference of the transfer function, ΔT, is calculated as

$$\Delta T = \int_{0.05}^{1} T_{noWEC} - T_{WEC}\, df \tag{3}$$

and shown in Table 2. Test 3 showed the largest decrease of the transfer function because the energy in the transfer functions was highest in Test 3 and the WEC buoy transfer function was consistently lower than the no WEC buoy transfer function across the frequency range. The transfer functions were also not constant across the six buoy tests for either the WEC-buoy or the no WEC-buoy. This implies that the amount of energy transferred between the waves and the buoys was not constant across the tests. The varying weight and heave plate configurations could have contributed to the variation, but tests 3, 5, and 6 all had identical weight and heave plate configurations and the transfer functions were still not constant. The transfer of energy between the waves and the WITT buoy depends not only on the response of the hull and heave plate to the waves but also on the response of the pendulums inside the buoy to the tilt of the hull and the tug of the heave plate bridle. Steep waves may push on the hull in an attempt to cause it to tilt but the pendulums inside the hull move, which causes the momentum to be transferred to the pendulums instead of the hull thereby decreasing the buoy tilt. The amount of momentum that can be transferred to the pendulums also depends on the pendulums resistance, which is affected by the current charge state of the battery that is connected to the generator. Further testing and controller development would be needed to characterize the transfer function across relevant wave states and WEC operating parameters.

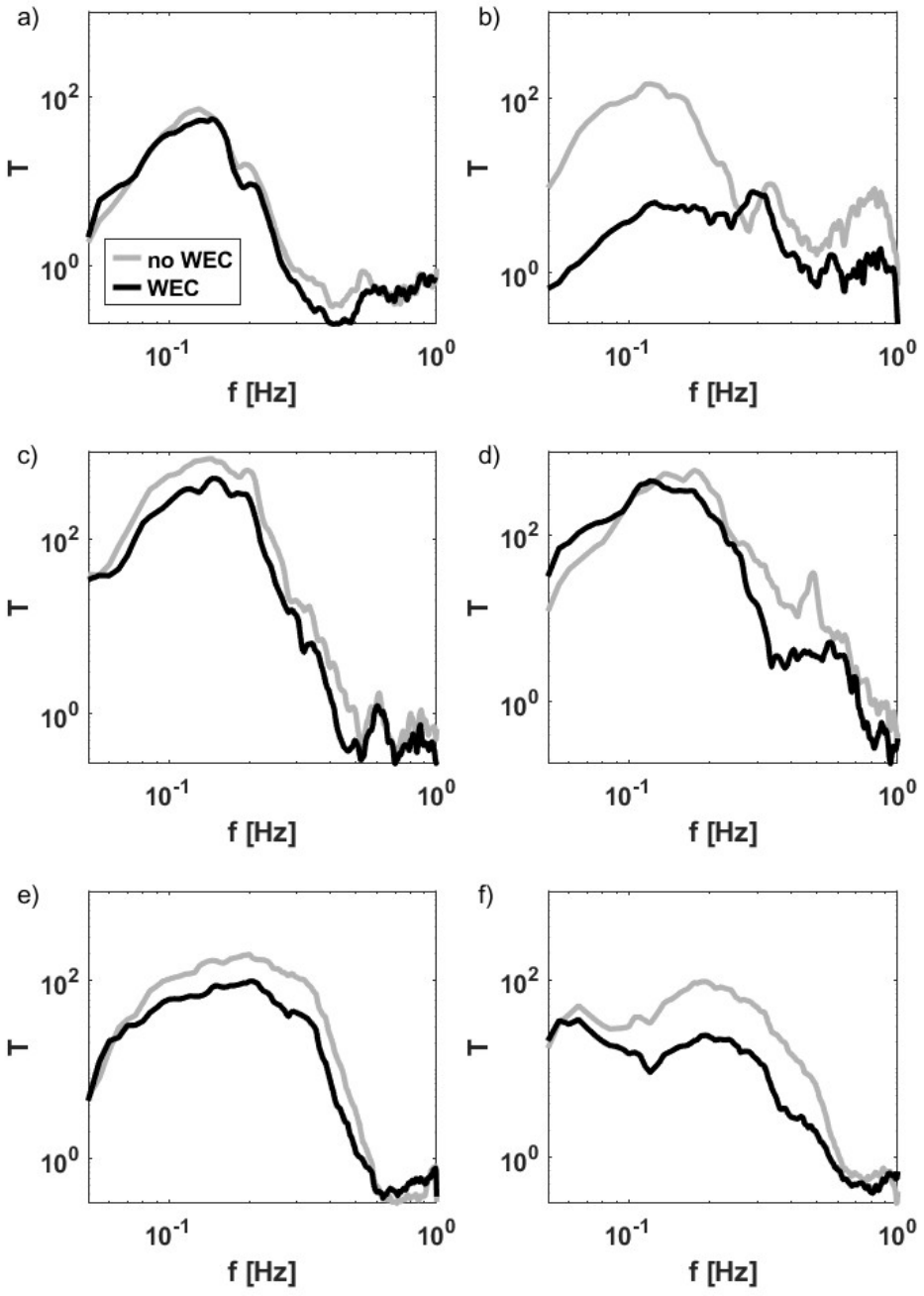

Figure 8. Transfer function, T, for the buoy with no WEC and the buoy with the WEC for the six tests. a) Test 1 on July 28, b) Test 2 on August 14, c) Test 3 on August 14, d) Test 4 on August 14, e) Test 5 on September 7, and f) Test 6 on September 7.

5.0 Discussion and Conclusions

A field study was conducted to investigate the effects of a WEC on buoy motion to determine if WECs can be a useful power source for wave measurement buoys. Six deployments tested the hypothesis that the momentum from the WEC pendulums would alter the buoy motion. Two identical buoys were purchased, and a WEC was mounted in one of them. Stationary weights were mounted in the second buoy, and the buoys were deployed with varying heave plate and external weight configurations. The field tests showed that both the WEC and heave plate/external weight configuration significantly altered the buoy motion. Spectral analysis showed that the addition of the WEC decreased the motion of the buoy in most cases. The decreased buoy motion was likely due to the WEC pendulums countering the buoy's response to the waves. The energy was not decreased by the addition of the WEC for high frequencies (>0.5 Hz) in the tests with the heave plate attached. The high-frequency motion may have been related to the natural frequency of the rubber cord/heave plate system and may have not had sufficient energy to activate the WEC pendulum system.

The results of the field study showed that configuring a buoy with a WEC, as well as the energy extraction capabilities of the WEC itself, are all counterproductive to accurately measuring waves. The configuration required to maximize the utility of the WEC was one that maximized buoy motion. The moving parts of the WEC extracted energy from the buoy and decreased its motion as compared to the no WEC-buoy. Wave statistics are commonly calculated from "wave following" buoys, and the requirements for a buoy-based WEC will likely not allow for accurate wave following, especially if WEC designers are pursuing wave resonance. With an empirically defined transfer function, the heave spectrum can be corrected to accurately estimate the wave parameters from a wave buoy (Teng 2002). However, while traditional wave buoys utilize a constant transfer function, it is likely that a series of transfer functions would need to be defined as a function of the wave state to fully characterize the effect of the WEC on the buoy motion. The appropriate transfer function would need be applied for each wave state to measure the waves in that wave state.

It is possible that an IRM WEC could be used to generate electricity on a larger wave measurement buoy where the WEC is much smaller than the buoy. Either the moving parts would have to be sufficiently small to avoid affecting the motion at the wave frequencies being measured, or the motion would need to be characterized with transfer functions for all wave states. The disadvantage of this scenario is that an IRM WEC with small moving parts may result in little to no energy harvested. Future field tests are needed to verify if small IRM WECs or an array of small IRM WECs can be used on a large wave measurement buoy without decreasing the buoy's ability to measure the waves.

This field study has revealed challenges to the usage of IRM WECs for power generation on wave measurement buoys that depend on the buoys' wave following nature to measure waves, but it has not decreased the value of IRM WECs for power generation on other types of buoys. Many oceanographic buoys measure variables other than wave conditions and those buoys may benefit from power production by an IRM WEC. The buoy that was used in this study is currently being used for water temperature studies in the Arctic and would benefit from a power generation system. The recent interest in the validation of marine carbon dioxide removal techniques will lead to the development of new sensors that will require large amounts of power at sea. The first use cases of WEC powered ocean observations should focus on metocean variables such as water temperature, air temperature, nitrogen, acoustics, light, wind speed, and barometric pressure. The need for WEC powered buoys is projected to increase with our need to monitor the changing climate and measure carbon fluxes.

References

Cavagnaro, R. J., A. E. Copping, R. Green, D. Greene, S. Jenne, D. Rose, and D. Overhus (2020). Powering the Blue Economy: Progress Exploring Marine Renewable Energy Integration with Ocean Observations. *Marine Technology Society Journal 54*(6), 114–125.

Cotter, E. D. and J. R. McVey (2021). Critical Interference Mechanisms for Marine Renewable Energy-Powered Ocean Observing Platforms. Technical report, Pacific Northwest National Laboratory PNNL-31985. Richland, WA.

Crowley, S., R. Porter, D. J. Taunton, and P. A. Wilson (2018). Modelling of the WITT Wave Energy Converter. *Renewable Energy 115*, 159–174.

Kenny, C. and J. McNally (2022). Internal Reaction Mass Taxonomy and Narrow-Down Study. Technical report, National Renewable Energy Laboratory NREL/PR-5700-83992. Golden, CO.

Klise, K., R. Pauly, K. M. Ruehl, S. Olson, T. Shippert, Z. Morrell, S. Bredin, C. Lansing, M. Macduff, T. Martin, C. Sivaraman, B. Gunawan, and F. Driscoll (2020). MHKiT (Marine and Hydrokinetic Toolkit) - Python. [Computer Software] `https://doi.org/10.5281/zenodo.3924683`.

Raghukumar, K., G. Chang, F. Spada, C. Jones, T. Janssen, and A. Gans (2019). Performance Characteristics of "Spotter," a Newly Developed Real-Time Wave Weasurement Buoy. *Journal of Atmospheric and Oceanic Technology 36*(6), 1127–1141.

Teng, C.-C. (2002). Wave Measurements from NDBC Buoys and C-MAN Stations. In *OCEANS'02 MTS/IEEE*, Volume 1, pp. 517–524. IEEE.

Wickett, M. J., S. Hindley, and M. B. Wickett (2019). WITT: Harvesting Energy From Subsea, Vortex-Induced Vibration. *Marine Technology Society Journal 53*(4), 17–25.

Pacific Northwest National Laboratory

902 Battelle Boulevard
P.O. Box 999
Richland, WA 99352
1-888-375-PNNL (7665)

www.pnnl.gov